Comparison of Lumped Simulation Models for Three Different Building Envelopes

Kyung-Soo Yoon
Home Appliance Air-Conditioning
LG Electronics
Seoul, South Korea
Kyungsoo.yoon@lge.com

Young-Jin Kim and Cheol-Soo Park
Dept. of Architectural Engineering
SungKyunKwan University
Suwon, South Korea
cheolspark@skku.ac.kr

Keon-Ho Lee
Dept. of Building Research
Korea Institute of Construction Technology
Goyang, South Korea
lee1ncdh@kict.re.kr

***Abstract*—Over the last several decades, shading devices such as blinds, louvers, roll shades, etc., have received much attention due to their roles as indoor environmental controllers (preventing glare, blocking shortwave radiation, and contributing to thermal comfort). In order to allow the aforementioned systems to act as true *optimal* controllers, a fast and accurate mathematical model that is able to predict the dynamic behavior of the system is necessary. This paper describes the development of a lumped simulation model of an indoor blind system adjacent to double glazing (6 mm clear+12 mm air + 6 mm low-e). This is typical of office building shading systems in Korea. Rather than attempting to develop the most detailed and accurate model of the system, the approach described in this paper is based on the postulated *minimalistic* model augmented with a parameter estimation technique. The lumped simulation model was validated with measurements obtained from an in-situ, full-scale experimental facility mounted on the south-facing façade. It was found that the calibration method delivers accurate results for the unknown parameters (convective heat transfer coefficients and air permeability of the shading device), allowing the calibrated lumped model to be used in ensuing optimal control and performance studies.**

Keywords-blind; lumped model; parameter estimation; calibration; validation.

I. INTRODUCTION

Saving energy through architectural design is an important issue due to climate change and high oil prices. In particular, interests in building envelope design, control, and performance assessment are increasing due to the impacts on building energy and comfort. The latest trend in envelope systems is to increase window area for transparency and aesthetics. However, this leads to undesired heat gain/loss, assymetric discomfort, and an increased energy consumption. Therefore, shading devices are often adopted to reduce the aforementioned problems. Shading devices installed indoors, outdoors, or in cavities have several effects on indoor environmental conditions (preventing glare, blocking shortwave radiation, and contributing to thermal comfort).

The development of simulation model, optimal control, and energy performance assessment studies for the following three envelope systems are now in progress by the authors. System I is a generic type used in a curtain wall system. Systems II and III are examples of the double-skin with different configuration (cavity depth, blind slat, etc.)

- System I: double glazing (low-e) + interior blind system (blind slat 50mm)
- System II: double-skin (50 mm cavity) system, blind slat 15mm
- System III: double-skin (200 mm cavity) system, blind slat 50mm

In order to assess the energy performances of the systems, it is necessary to develop a simulation model. Obviuosly, the developed simulation model can be used later in optimal design and control studies. In particular, the simulation model should be able to predict the behavior of the system quickly and accurately in order to apply optimal control.

There are three approaches to mathematically modeling a system: (1) the use of a 3D, full-blown model, (2) the use of a whole building simulation tool (Energy Plus, Esp-r, TRNSYS [1], IDA ICE [2], TAS [3], etc.), and (3) the use of a lumped simulation model.

The first approach divides the system into small nodes in the form of a grid, and then mathematically expresses the heat and mass transfers that appear in each node. While this approach has the advantage of precisely modeling the airflow dynamics and temperature distribution around the system, the mathematical modeling requires numerous assumptions as well as detailed information. For these reasons, the uncertainty of its simulation results might increase.

The second approach is to use a general-purpose tool developed for analyzing performance of a whole building. While this approach is advantageous in terms of assessing the influence of the envelope system on the performance of the entire building, it has a limited ability to express in detail the physical phenomena that involve transient convective and radiant heat transfer and airflow movement in and around the system. It is difficult to make accurate predictions about the airflow movement in a cavity [4], and it is not easy to apply modern control strategies (Pontryagin's minimum principle [5], the Hamilton-Jacobi-Bellman equation [5], a Riccati equation [5]), to any shading installed device (control of louver slat angles, ventilation dampers in the cavity, etc. because of high nonlinearity of the system.

The third approach is to express the fundamental heat transfer phenomenon in a system as one-dimensional (1D) in a lumped fashion. As a result, this model has the advantage of fast calculations. For real-time performance optimization of a system, this approach can be applied for optimal control and performance assessment. In other words, it is possible to optimize and assess system performance by determining the optimal variables in real-time [6].

The purpose of the paper is to present the initial development of the System I (Fig. 1) among the aforementioned three systems. In this study, the third approach was employed and the heat transfer and airflow movement are expressed in a 1D state-space equation. The lumped simulation model was calibrated using the parameter estimation technique. Next, it was experimentally validated with the test facility described in the following section.

This paper reports the following three processes for development of the lumped simulation model of System I.

- Step 1 (mathematical modeling): modeling complex heat transfer and airflow movement in the system
- Step 2 (calibration): estimating unknown parameters in the model
- Step 3 (validation): comparing simulated results with measurements.

II. EXPERIMENT SETUP

An experimental test facility of the system was constructed in an actual building as shown in Fig. 2. The installed system faces true South and the window was double glazing (6 mm clear glazing + 12 mm air space + 6 mm low-e glazing), and the blind was placed adjacent to the indoor glazing. The blind was 10 cm from the surface of the interior pane, its height was 150 cm from the bottom to the top of the pane, and the width of the blind slat was 5 cm. The control of the slat angle was performed by an electric motor.

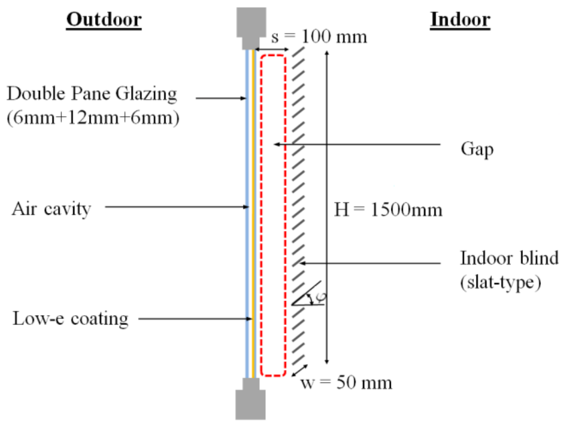

Figure 1. System I (24 mm double-glazing + interior blinds).

(a) Elevation (b) Interior

Figure 2. The test unit installed on Sungkyunkwan University campus, Korea.

Fig. 3 shows the elevation and section of the experiment unit, the locations of the sensors, and the measurement instruments used for study. Wind speed and wind direction were measured using a wind sensor (Wind Sonic, Gill inc.). Direct and diffuse solar radiation was measured using a pyranometer (S-LIB-M003, HOBO inc.). The outdoor humidity was measured using a hygrometer (M-RSA, HOBO inc.). T-type thermocouples were installed at three points vertically, as shown in Fig. 3, to measure glazing surface, gap air, and indoor temperatures. The data were collected using a National Instrument data logger.

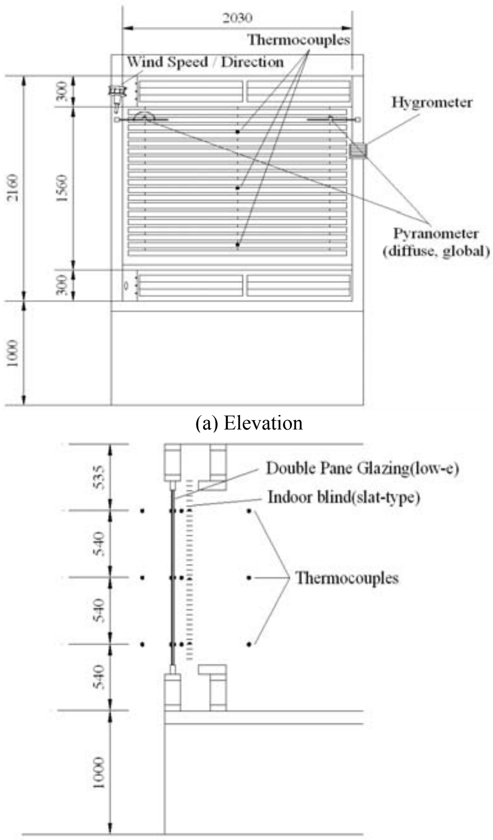

(a) Elevation

(b) Section

Figure 3. Elevation and section of the experiment unit and the locations of the sensors (unit: mm).

III. Mathematical Model

In order to describe the dynamics of the indoor blind system, the governing heat and mass transfer phenomena were studied as follows: 1) direct, diffuse, and reflected solar radiation; 2) long wave radiation between surfaces; 3) convective heat transfer along the exterior and interior glazing surfaces and blind slats; and 4) air movement through the gap (between the glazing and the indoor blinds).

In this study, the heat transfer and airflow phenomena in the system were described in a lumped fashion. The essence of the lumped model is based on the assumption that the temperature of the solid is spatially uniform at any instant during the transient process [7]. With this in mind, a one-dimension model without a temperature gradient was assumed (Fig. 4) in order to describe the simplified dynamics of a three-dimensional (3D) system. $x1$-$x5$ are state variables which represent the temperature at each point in Fig. 4. Although this approach does not render explicit information about the vertical and horizontal temperature gradients, it is assumed to be sufficient to represent the overall thermal characteristics of any indoor blind system and, in particular, to determine the optimal control actions. This assumption has to be substantiated by experiments and will be described later in the paper.

For the details of the grey-box approach and the thermal model, see [8] [9].

This paper gives a detailed account of the airflow occurring in the gap shown in Fig. 4. The size of the space between the blind tip and the window (gap in Fig. 4) has an effect on the energy performance of the system [10]. Therefore, the gap is equated with a cavity in this study.

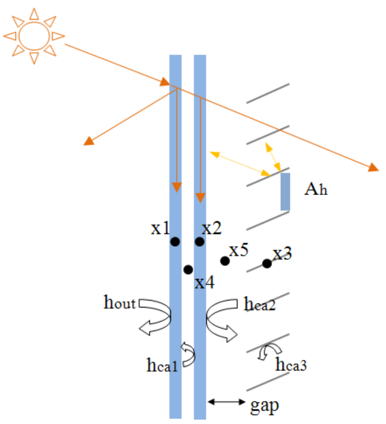

Figure 4. Simplified system (● = state variables, x1= outer glazing temperature of the double-pane, x2= inner glazing temperature of the double-pane, x3= louver slat temperature, x4= cavity air temperature in the double-pane, x5= air temperature in the gap).

Airflow in the gap is caused by a difference between the gap temperature (T_{gap}) and the indoor air temperature (T_{in}). The effects of the blinds (blind slat angle, distance from the glazing surface, etc.) also affect this airflow. The presence of the blind has a strong effect on the heat transfer from the indoor glazing. Moreover, when blind slats are fully closed (90°), the air velocity and convective transfer are promoted by the fully closed cavity effect [10].

In general, the airflow speed in the gap (Fig. 4) can be expressed in (1) [11] [12].

$$v_{gap} = \frac{\left[\left(\left(\frac{12\mu H}{s^2}\right)^2 + \frac{2\rho^2(1+z_{in}+z_{out})\rho_0 T_0 gH\sin\theta\left|T_{in}-T_{gap}\right|}{T_{in}T_{gap}}\right)^{\frac{1}{2}} - \frac{12\mu H}{s^2}\right]}{\rho(1+z_{in}+z_{out})} \tag{1}$$

where v_{gap} is the air velocity in the gap in m/s, μ is the viscosity of the gap air at temperature (T_{gap}) in NS/m^2, ρ is the air density in the gap in kg/m^3, Z_{in} is the inlet pressure drop factor, Z_{out} is the outlet pressure drop factor, T_0 is the reference temperature in K, ρ_0 is the density of air at temperature T_0 in kg/m^3, g is the acceleration due to gravity in m/s2, and θ is the tilt angle of the window in degrees (0° = horizontal, 90° = vertical).

Z_{in} and Z_{out} of (1) can be calculated using (2) and (3) [12].

$$z_{in} = \left[\frac{A_{gap}}{0.66\left(A_{bot}+\frac{A_{top}}{2(A_{bot}+A_{top})}(A_l+A_r+A_h)\right)}-1\right]^2 \tag{2}$$

$$z_{out} = \left[\frac{A_{gap}}{0.60\left(A_{top}+\frac{A_{bot}}{2(A_{bot}+A_{top})}(A_l+A_r+A_h)\right)}-1\right]^2 \tag{3}$$

where A_{gap} is the cross-sectional area of the gap in m^2, A_{top} is the area of the top opening in m^2, A_{bot} is the area of the bottom opening in m^2, A_l is the area of the left-side opening in m^2, A_r is the area of the right-side opening in m^2, and A_h is the air permeability of the shading device in m^2.

The air permeability of the shading device (A_h, Fig. 4) changes according to the configuration of the shading layer (roll shade, screen or blind, etc.). In the case of the blinds, A_h varies with the blind slat angle. Based on the descriptions given above, the mathematical model was expressed with a state-space equation, as shown in (4).

$$\dot{x} = A(u,t)x + b(u,t) \tag{4}$$

where x is the state variable vector, A is the state matrix, u is the input vector, and b is the load vector.

IV. COMPARISON BETWEEN SIMULATED AND PRIMARY MEASURED VALUES

For a comparison of the simulated and measured values, the first experiment was conducted for about 108 hours (Jul 27, 2009 - Aug 30, 2009). The data were recorded with a sampling time of one minute, and the number of measured data points was 6,412 (6,412 minutes = four days, ten hours, and 52 minutes). During the experiment, the internal temperature of the laboratory was set to 24 °C, and the slat angle (0° = horizontal, 45° = facing the floor, 90° = vertical) was changed randomly, as shown in Fig. 5 (c). Fig. 5 (a) and (b) show the recorded indoor and outdoor air temperatures and the solar radiation.

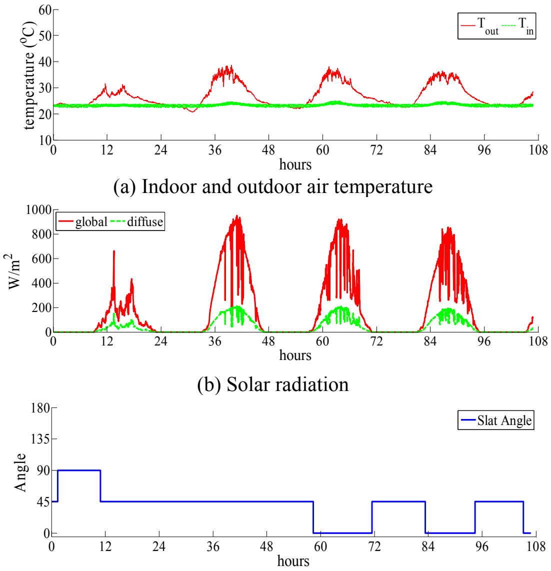

(a) Indoor and outdoor air temperature

(b) Solar radiation

(c) Slat angle

Figure 5. Weather conditions and slat angle of the primary experiment.

Table 1 shows the differences between the measured temperatures and predictions from the un-calibrated simulation model that use literature values of the convective heat transfer coefficients (h) and air permeability of the shading device (A_h) [7] [11] [13]. It should be noted that the air temperature ($x4$) of the small cavity in the double-pane was not measured.

As shown in Table 1, the temperature difference between the simulation and measurement was 1.91 °C. Considering a degree of details of the lumped model, the un-calibrated model has an unexpected accuracy (the T-type thermocouples used in the experiments had an accuracy range of ±0.5 °C). The differences between the simulated and measured values result from the unknown parameters of the model, the assumptions used in the modeling process, and the simplifications of the physical phenomena in the system (3D→1D).

TABLE I. DIFFERENCES BETWEEN THE SIMULATED AND MEASURED VALUES (UN-CALIBRATED MODEL).

$\lvert x_{measured}-x_{simulated} \rvert$	results (°C)
x_1	2.81
x_2	2.60
x_3	0.86
x_5	1.38
Average	**1.91**

Table 2 shows the convective heat transfer coefficient values of the un-calibrated model. In the case of the convective heat transfer coefficients (Table 2), the literature values [7] [14] [15] [16] are derived empirically from experiments under specific conditions (vertical walls instead of windows). The convective heat transfer coefficients are influenced greatly by surface roughness and geometry, system geometry (height, width, etc.), the local environment and the nature of the air motion. For these reasons, they should be calibrated to fit to the test unit ($h_{ca,1}$, $h_{ca,2}$, $h_{ca,3}$ in Fig. 4).

TABLE II. CONVECTIVE HEAT TRANSFER COEFFICIENTS OF THE UN-CALIBRATED (W/M²).

	Literature values	Literature
h_{out}	7.44	Reference [14]: smooth surface
	8.00	Reference [11]: summer conditions
	22.70	Reference [15] : summer conditions
$h_{ca,1}$	0.60	Reference [7]: the convective heat transfer coefficient when both ends of the wall were insulated, allowing only horizontal heat flow conditions
$h_{ca,2}$	2.42	Reference [12]: the convective heat transfer coefficient for the vertical cavity with a shade layer (shade, screen, blind)
$h_{ca,3}$	4.16	Reference [7]: the convective heat transfer coefficient for an isothermal horizontal cylinder

The air permeability of the shading device (A_h) depends on the blind slat angle, and it is difficult to measure accurate air permeability . Even in the fully closed position (vertical, 90°), there is air permeability through openings between blind slats. Such air permeability has an influence on airflow in the gap.

Thus, the unknown parameters related to the convective heat transfer coefficients and the airflow must be identified with a suitable parameter estimation technique based on extensive data points obtained from experiments. This will be discussed in the following sections.

V. CALIBRATION

The parameter estimation technique is used to determine unknown parameters that minimize the differences between the actual measurements and the simulation predictions [8]. This approach is used to estimate values that cannot be calculated analytically or measured directly. The parameter estimation technique can be expressed as the minimization of the objective function (S), as in (5).

 ISBN: 978-1-61208-234-9

$$\min\ S = \sum_{k=1}^{z} \left[Y_k - \psi_k\left(\xi_i\right)\right]^T \left[Y_k - \psi_k\left(\xi_i\right)\right] \quad s.t.:\ lb \le \xi \le ub \tag{5}$$

where Y_k is the observation vector, ψ_k is the discrete state vector in discrete state space, z is the number of observations, ξ is a vector of the unknown parameters, lb is the lower bound of the unknown parameters, and ub is the upper bound of the unknown parameters.

In this study, the aforementioned convective heat transfer coefficients (Fig. 4) and the air permeability of the shading device, given by (2) and (3), were selected as the unknown parameters.

Equation (1) is orginally developed for the shade layer (e.g., roll shades) and needs calibration to be used for the indoor blind system installed in the experimental unit. In other words, air permeability of the shading device should be estimated because it cannot be calculated exactly, and it should be determined based on the blind slat angle. The selected unknown parameters are expressed in the following equations.

$$h_{out} = 5.678\left[\xi_1 + \xi_2\left(\frac{u_{lsv}}{0.3048}\right)^{\xi_3}\right] \tag{6}$$

$$h_{ca,1} = \frac{N \cdot k_f}{D_s} + \xi_4 \tag{7}$$

$$h_{ca,2} = \xi_5 + \xi_6\left(\Delta x\right)^{\xi_7} + \xi_8\left(u_{ca}\right)^{\xi_9} \tag{8}$$

$$h_{ca,3} = \xi_{10} + \xi_{11}\left(\Delta x\right)^{\xi_{12}} + \xi_{13}\left(u_{ca}\right)^{\xi_{14}} \tag{9}$$

$$\begin{aligned} &A_h = a_1\xi_{15} + a_2\xi_{16} + a_3\xi_{17} \\ &If\quad \varphi_{slat} = 0^\circ,\ a_2 = a_3 = 0,\ a_1 = 1 \\ &If\quad \varphi_{slat} = 45^\circ,\ a_1 = a_3 = 0,\ a_2 = 1 \\ &If\quad \varphi_{slat} = 90^\circ,\ a_1 = a_2 = 0,\ a_3 = 1 \end{aligned} \tag{10}$$

where u_{lsv} is the local surface velocity in m/s, N is the Nusselt number [dimensionless], k_f is the thermal conductivity of the glazing in W/mK, D_s is the cavity width of the double-pane in m, ξ represents the unknown parameters, Δx is the temperature difference in K, and a is a constant.

Equation (6) is empirically driven for the convective heat transfer coefficient of exterior surfaces (h_{out}) [14]. The purpose of ξ_4 in (7) is to account for the end effect. Equations (8) and (9) are mathematical representations of the convective heat transfer coefficients in the gap, and they are expressed as functions of airflow velocity and temperature difference (the pane surface and gap air temperatures). Simply put, Equations (8) and (9) can be read as a consideration of the convective effects according to airflow velocity and temperature difference.

The air permeability of the shading device (A_h) from (2) and (3) was expressed in (10) and also reflects the changes due to the blind slat angle (φ_{slat}).

The function LSQNONLIN in the MATLAB optimization toolbox was used to solve (5). LSQNONLIN is specially suited for this kind of constrained nonlinear optimization problem. The values of the unknown parameters were numerically estimated using LSQNONLIN. Table 3 shows the estimated convective heat transfer coefficients. There are considerable differences in convective heat transfer coefficients between the un-calibrated (Table 2) and calibrated models (Table 3). The calibrated value (h_{out}) in Table 3 is similar to the summer conditions in [15] (Table 2).

For $h_{ca,1}$, the estimated values were greater than those in the literature because the literature values are derived empirically from experiments under specific conditions (both ends of the wall are insulated, allowing for only horizontal heat flow). In other words, the literature values do not take into consideration the lateral heat loss that occurs in the cavity, and they are usually valid for solid walls, but not for transparent glazing.

For $h_{ca,2}$, the estimated values were also greater than those calculated from the literature.

In counterpoint to the literature value for the shading layer, our study took into account variations in the airflow based on the blind slats. The differences in $h_{ca,2}$ were due to uncertain air movement in the gap (Tables 2, 3). $h_{ca,3}$ was close to that of the literature.

TABLE III. CONVECTIVE HEAT TRANSFER COEFFICIENTS OF THE CALIBRATED MODEL (W/M^2).

	Estimated values
h_{out}	24.52
$h_{ca,1}$	4.51
$h_{ca,2}$	8.23
$h_{ca,3}$	4.04

The estimated unknown parameters (ξ_1 - ξ_{15}) were applied to the simulation model and compared with the measured values (Fig. 6, Table 4). After calibration, the average difference between the simulated and measured temperatures was 1.13 °C (Table 4). It is clear from the results that the accuracy of the calibrated model was improved compared to that of the un-calibrated model. Furthermore, the estimated air permeability of the shading device depends on the blind slat angle (Table 5). The A_h for slat angles of φ = 45° (facing the floor) was greater than the A_h for slat angles of φ = 0° (horizontal). The A_h calculated using the calibrated results implies explicit conditions about the influence of the air permeability and the airflow configuration based on the slat angles and the impact of the convective heat transfer at the indoor glazing surface. That is, an ascending airflow is promoted by buoyancy (compared with the horizontal conditions) when φ =45°. This effect increases the convective heat transfer adjacent to the internal glazing surface.

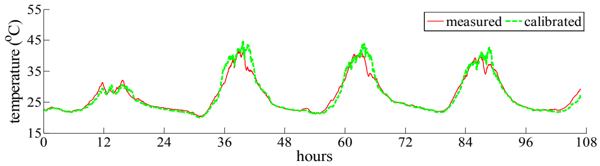

(a) Outer glazing of the interior double-pane (x_1)

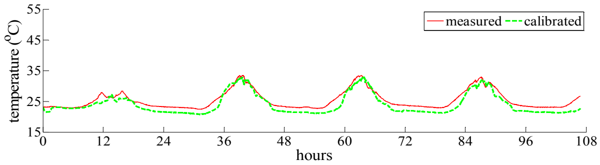

(b) Inner glazing of the interior double-pane (x_2)

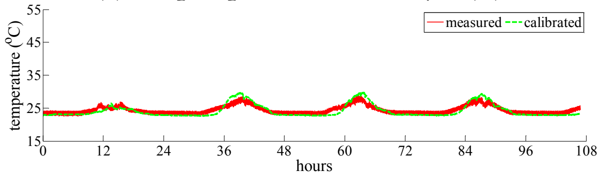

(c) Blind slat (x_3)

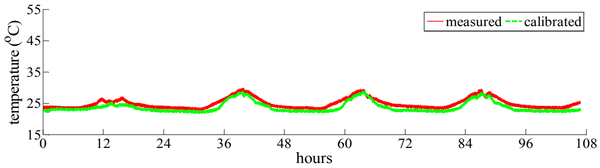

(d) Gap between glazing and blind (x_5)

Figure 6. Comparison of the simulated and measured values for the calibrated model.

TABLE IV. DIFFERENCES BETWEEN THE SIMULATED AND MEASURED VALUES FOR THE CALIBRATED MODEL.

$\lvert x_{measured}-x_{simulated} \rvert$	**results (°C)**
x_1	0.88
x_2	1.50
x_3	0.90
x_5	1.23
Average	**1.13**

TABLE V. AIR PERMEABILITIES OF THE SHADING DEVICE.

	results (m2)
0°	2.29
45°	3.90
90°	0.82

VI. VALIDATION

Validation processes were performed to determine whether the calibrated model was capable of accurately predicting the system's response. To validate the model, the second experiment was conducted for about 132 hours (Aug 1, 2009 - Aug 6, 2009). The data were recorded with a sampling time of one minute, and the number of measured data points was 7,874 (7,874 minutes = five days, 11 hours, 14 minutes). The measured values were compared with the predicted values from the calibrated model. Fig. 7 shows the recorded indoor and outdoor air temperatures and the solar radiation.

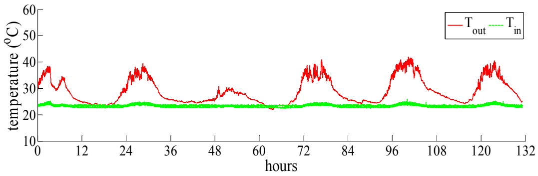

(a) Indoor and outdoor air temperatures

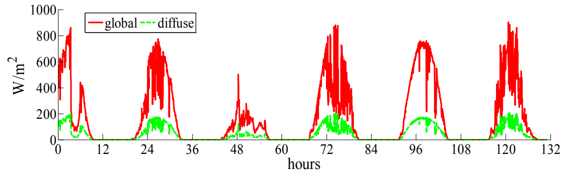

(b) Solar radiation

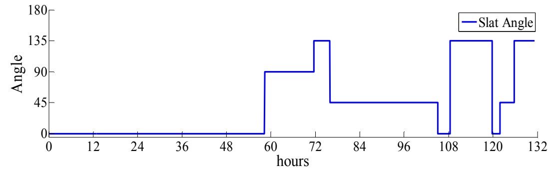

(c) Slat angle

Figure 7. Weather conditions and slat angles of the second experiment.

Fig. 8 shows a comparison of the simulated and measured values, and Table 6 shows the average differences in temperature between the simulated and measured state variables. The overall average temperature differences were 1.27 °C. Considering the accuracy range (±0.5 °C) of the thermocouples (Omega T-type), the calibrated model proved surprisingly accurate in the prediction of the most relevant state variables.

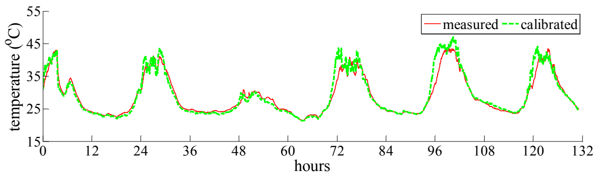

(a) Outer glazing of the interior double-pane (x_1)

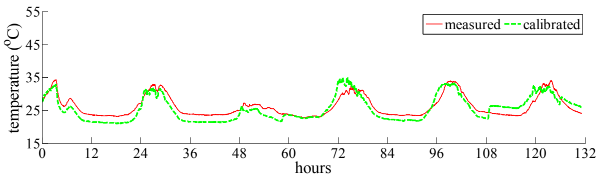

(b) Inner glazing of the interior double-pane (x_2)

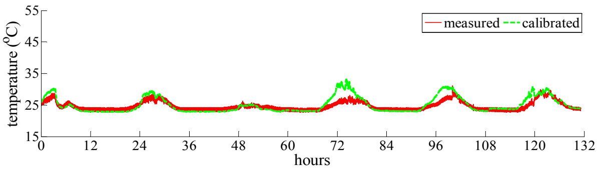

(c) Blind slat (x_3)

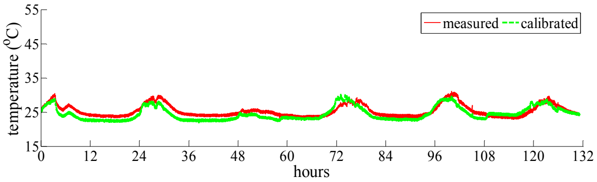

(d) Gap between the glazing and the blind (x_5)

Figure 8. Validations of the state variables.

TABLE VI. RESULTS OF VALIDATION FOR THE CALIBRATED MODEL (STATE VARIABLES).

$\lvert x_{measured}-x_{simulated}\rvert$	**results (°C)**
x_1	1.02
x_2	1.79
x_3	1.02
x_5	1.24
Average	**1.27**

Table 7 shows the calculated convective heat transfer coefficients using the estimated unknown parameters. As mentioned above, there are many differences from the literature values (Table 2).

TABLE VII. RESULTS OF VALIDATION FOR THE CALIBRATED MODEL (CONVECTIVE HEAT TRANSFER COEFFICIENTS).

	Estimated values
h_{out}	24.25
$h_{ca,1}$	4.52
$h_{ca,2}$	9.60
$h_{ca,3}$	4.56

Fig. 9 shows the air velocity (v_{gap}) in the gap calculated using (1). The average air velocity was 15 cm/s, with a maximum value of 36 cm/s.

Considering the air velocity in the gap, the convective heat transfer phenomenon depends on airflow movements in the gap. In other words, air velocity is influenced by gap size and configuration. This indicates the need of model calibration based on the system configuration and the components in envelope system.

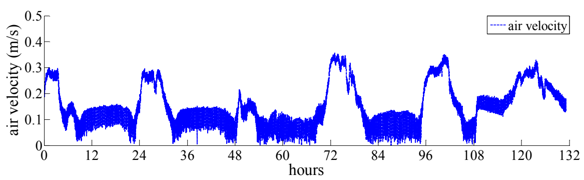

Figure 9. *Air velocity between the glazing and the blind (gap).*

VII. CONCLUSION AND FUTURE WORK

This study attempted to develop a simplified model for real-time optimal control and performance assessment of an indoor blind system. The unknown parameters in the mathematical model were estimated using a parameter estimation technique. The model was validated, implying that the mathematical model developed for this study is capable of accurately predicting system response. Based on the results of this study, the following conclusions can be made.

- Use of the lumped model: 3D modeling of heat transfer and airflow movement in a system is complicated, but the lumped model, expressed in one-dimension (1D), is a practical approach for predicting system behavior. Evidently, the 1D lumped model is also able to express the behavior of a system using a calibration technique.
- The unknown parameters: the un-calibrated model (using values from the literature) can be improved into a more accurate calibrated model using the parameter estimation technique. Namely, it was shown that there are limitations in developing a simulation model based solely on the parameters from the literature.
- Performance assessment and real-time optimal control: the simulation run-time was as short as several seconds using the calibrated model. The lumped model has the advantages of fast calculation, flexibility, etc., for emulating optimal control. The lumped simulation model can be applied to performance assessment and real-time optimal control.
- The airflow movement in the gap: it is necessary to consider airflow movement in the gap if a slat-type of indoor blinds are installed. Air permeability of the shading device (A_h) was estimated using the parameter estimation technique and was consequently adjusted according to the blind slat angle. Thus, the size and component of the gap are always of concern for modeling indoor blind systems since the airflow movement in the gap also changes with the blind slat angle.

Based on the results of this study, following studies are on-going.

- Optimal control and performance assessment: optimal control and performance assessment in cooling, heating, and intermediate modes, under differentweather conditions (clear, overcast), and orientations.
- Integrating of the lumped model with a whole building simulation model: the lumped model is applied to optimal control study, and the whole building simulation model is used to confirm the effect of the optimal control on the whole building energy performance.

 ISBN: 978-1-61208-234-9

- Applicability of the lumped model: the mathematical model of the double-skin system should be calibrated according to system configuration, local environment, components such as cavity width, cavity depth, cavity height, louver materials (reflectance, color, thickness, width, and geometric size), glazing type, etc. [9]. Subsequently, it is necessary to investigate the applicable range of the lumped model.

ACKNOWLEDGMENT

This research is supported by a grant (11 High-tech Urban G02) from High-Tech Urban Development Program funded by the Ministry of Land, Transport and Maritime Affairs of the Korean Government.

REFERENCES

[1] http://www.trnsys.com/

[2] http://www.equa.se/ice/intro.html

[3] http://www.edsl.net/main/

[4] O. Kalyanova, P. Heiselberg, C. Felsmann, H. Poirazis, P. Strachan, and A. Wijsman, "An empirical validation of building simulation software for modelling of double skin facade(DSF)," Proceedings of the 11th IBPSA Conference (International Building Performance Simulation Association), July 27-30, Glasgow, Scotland, 2009, pp. 1107-1114.

[5] F. L. Lewis, and V. L. Syrmos, "Optimal Control," John Wiley & Sons, 2nd ed. 1995.

[6] C.S. Park, G. Augenbroe, N. Sadegh, T. Messadi, and T. Messadi, "Occupant Responsive Optimal Control of Smart Facade Systems," 8th International IBPSA Conference, Eindhoven, Netherlands, 2003, pp. 1009-1016.

[7] F.P. Incropera and D.P. DeWitt, "Fundamentals of heat and mass transfer," John Wiley & Sons, 6th ed., 2007

[8] C.S. Park, G. Augenbroe, T. Messadi, and M. Thitisawat, "Calibration of a lumped simulation model for double-skin facade systems," Energy and Buildings. vol. 36. 2004, pp. 1117-1130.

[9] S.H. Yoon, and C.S. Park, "State-space Approach for Lumped Modeling of Double-skin System," Proceedings of the Sustainable Building Conference 2007 Hong Kong (SB07 HK), December 3-5, Hong Kong, China, 2007

[10] D. Naylor, and H. Shahid, "Energy performance of a window with a horizontal venetian blind," Energy and Buildings, vol. 37. 2005, pp. 836-843.

[11] ISO, "Thermal performance of windows, doors, and shading devices - Detailed calculations," ISO 15099, 2003

[12] DOE, "Energy Plus Engineering Reference: The Reference to EnergyPlus Calculations," US Department Of Energy, 2009

[13] S. Rheault, and E. Bilgen, "Heat Transfer Analysis in an Automated Venetian Blind Window System," Journal of Solar Energy Engineering, vol. 111. no. 1. 1989, pp. 89-95.

[14] J.A. Clarke, "Energy Simulation in Building Design," Butterworth-Heinemann, 2nd ed., 2001

[15] ASHRAE, "ASHRAE handbook fundamentals". ASHRAE. Atlanta. USA, 2005

[16] W.H. McAdams, "Heat Transmission," New York: McGraw-Hill, 1954.